

A&A manuscript no.
(will be inserted by hand later)

Your thesaurus codes are:

11.04.2; Galaxies: dwarf 11.09.1; M81 Group 11.16.1; Galaxies: photometry

ASTRONOMY
AND
ASTROPHYSICS

Dwarf Spheroidal Galaxies in the M81 Group Imaged with WFPC2 ^{*}

I.D.Karachentsev¹, V.E.Karachentseva², A.E.Dolphin³, D.Geisler⁴, E.K.Grebel^{5,6**},
P.Guhathakurta^{7***}, P.W.Hodge⁵, A.Sarajedini⁸, P.Seitzer⁹, and M.E.Sharina¹

¹ Special Astrophysical Observatory, Russian Academy of Sciences, N.Arkhiz, KChR, 357147, Russia,

² Astronomical observatory of Kiev University, 04053, Observatorna 3, Kiev, Ukraine

³ Kitt Peak National Observatory, National Optical Astronomy Observatories, P.O. Box 26732, Tucson, AZ 85726, USA

⁴ Departamento de Fisica, Grupo de Astronomia, Universidad de Concepcion, Casilla 160-C, Concepcion, Chile

⁵ Department of Astronomy, University of Washington, Box 351580, Seattle, WA 98195, USA

⁶ Max-Planck-Institut für Astronomie, Königstuhl 17, D-69117 Heidelberg, Germany

⁷ UCO/Lick Observatory, University of California at Santa Cruz, Santa Cruz, CA 95064, USA

⁸ Astronomy Department, Wesleyan University, Middletown, CT 06459, USA

⁹ Department of Astronomy, University of Michigan, 830 Dennison Building, Ann Arbor, MI 48109, USA

Received:16 May 2000

Abstract. We obtained HST/WFPC2 images of the dwarf spheroidal (dSph) galaxies K61, K63, K64, DDO78, BK6N, and kk77 in the M81 group. Our color-magnitude diagrams show red giant branches with tips (TRGB) falling within the range of $I = [23.8 - 24.0]$ mag. The derived true distance moduli (DM) of the 6 dSphs ranging from 27.71 to 27.93 mag are consistent with their membership in the group. Given accurate distances of 5 other group members, which have been derived via TRGB or cepheids, the mean DM of the M81 group is (27.84 ± 0.05) mag. We find the difference of the mean distances to the M81 and NGC 2403 groups to be $D_{M81} - D_{NGC2403} = (0.5 \pm 0.2)$ Mpc, which yields a deprojected separation of 0.9 Mpc. With respect to the Local group, M81 and NGC 2403 have radial velocities of 106 and 267 km s⁻¹ respectively, while the velocities of the group centroids are 142 and 281 km s⁻¹. The higher velocity of the closer system may indicate that these groups are moving towards each other, similar to the Milky Way and M31 in the Local group. Several globular cluster candidates have been identified in the galaxies.

Key words: : galaxies: dwarf spheroidal — galaxies: stellar content — galaxies: distances — galaxies: M81 group

1. Introduction

Until recently most studies of dwarf spheroidal galaxies have been carried out in the Local Group only. The properties of the Local Group sample have been reviewed by Grebel (1997), Da Costa (1998), and Mateo (1998). But now progress is being made in the study of the dwarf population of other nearby groups, such as the M81 group, thanks to the efforts of various authors. Being among the faintest galaxies and of very low surface brightness, dSphs are rather difficult to recognize optically in the sky. As gas-poor galaxies, they are usually undetectable in the HI line as well. In the case of the M81 group an additional observational difficulty arises, because of the group location in an area of the sky that is contaminated with dense Galactic HI emission (Appleton et al. 1993) and Galactic cirrus (Sandage 1976). Therefore, the only way to establish the true dwarf spheroidal membership in the M81 group is by measurement of their distances via photometry of their stellar populations. Below we briefly outline the history of discovery of dwarf spheroidal galaxies in the M81 group.

Van den Bergh (1959) published the DDO catalog of low surface brightness objects with angular diameters $a > 1'$ revealed by visual inspection of the POSS-I plates. In the vicinity of M81 he found a concentration of LSB galaxies, which he classified as irregulars and spheroidals. As a prototype of dSphs, the LG dwarf spheroidal system in Draco was chosen. Out of 13 supposed dwarfs in the vicinity of M81, the objects DDO 44, 71, 78, and 87 were classified as dSphs. Later van den Bergh (1966) ascribed them to luminosity class V, without morphological type indication. Later DDO 87 was detected in HI by Fisher and Tully (1975) and reclassified as dIrr.

Karachentseva (1968) made an independent visual all-sky survey of the POSS-I prints for probable Sculptor-type

^{*} Based on observations made with the NASA/ESA Hubble Space Telescope. The Space Telescope Science Institute is operated by the Association of Universities for Research in Astronomy, Inc. under NASA contract NAS 5-26555.

^{**} Hubble Fellow

^{***} Alfred P. Sloan Research Fellow

Fig. 1. Digital sky survey images of eight dwarf spheroidal members of M81 group. The field size is $6'$, North is up, and East is to the left.

Fig. 2. WFPC2 images of six dSph galaxies: kk077, K61, DDO 71, K64, DDO 78, and BK6N produced by combining the two 600 s exposures through the F606W and F814W filters. Each galaxy is centered in the WF3 chip (WF3-FIX mode). The arrows point to the North and the East. Globular cluster candidates are indicated by circles.

Fig. 3. R images of K61 (a) and K64 (b) obtained with the 6-m telescope with exposures of 1200 s. Both the images have about the same orientation (top is NE).

dwarf galaxies with an angular diameter limit of $0'.5$. Around M81 she found 14 objects, and some of the largest of them were identified with the DDO objects. New supposed dSphs were K59, K61, and K64 (= UGC 5442, Nilson 1973). Later Mailyan (1973) rediscovered the objects K61 (=Mai 47), DDO 71 (=Mai 49), and K64 (=Mai 50) on the POSS-I prints.

Börngen and Karachentseva (1982) carried out a special photographic survey with the 2-m Tautenburg Schmidt telescope to search for new dwarf galaxies in the M81 group. All previously known objects were confirmed, and some previously uncatalogued objects were found, in particular, BK2N (dSph/dE), BK5N (dSph), and BK6N (dSph).

To clarify the morphology of supposed dwarf members in the M 81 group, about 40 objects were imaged with the 6-m telescope (Karachentseva et al. 1985, hereafter Atlas). Due to their very low surface brightness and lack of a significant surface brightness gradient (in contrast to dE galaxies), as well as to the absence of bright knots (in contrast to dIrr galaxies), the galaxies DDO 44, BK2N, K59, K61, BK5N, DDO 71 = K63, K64, DDO 78, and BK6N were classified as spheroidal dwarfs. Later Karachentsev (1994) found on the POSS-II films a new object, An 0946+6745, also classified as dSph.

Using CCD data obtained with the Burrell Schmidt telescope at Kitt Peak Caldwell et al. (1998) found several probable dSph members of the M81 group. One of them, named F8D1, was confirmed as a new spheroidal dwarf companion of M81 via HST observations. Recently Karachentseva & Karachentsev (1998, hereafter kk-list) have performed all-sky visual inspection of the POSS-II films for nearby ($V_0 < 500 \text{ km s}^{-1}$) dwarf galaxy candidates. As probable dSph members of the M81 group, they included into the kk-list the following objects: DDO 44 (=kk61), An0946+6745 (=kk77), K61 (=kk81), DDO 71 (=kk83), K64 (=kk85), DDO 78 (=kk89), and BK6N (=kk91). The galaxies BK2N, and K59 were omitted as background objects because of their high HI velocities, and BK5N because of its having a small ($0'.5$) angular diameter. However, Caldwell et al. (1998) imaged BK5N with HST and showed that it is a true dwarf spheroidal galaxy belonging to the M 81 group. The same conclusion

has been drawn about DDO 44 based on HST observations (Karachentsev et al 1999).

In this paper we consider the six dSph candidates that have not been imaged so far with HST. We briefly review previous data and present new results based on our HST observations, which allow membership in the M81 group to be established. Digital Sky Survey images of these galaxies are shown in Fig. 1, where the size of each square is $6'$. At the bottom of Fig. 1 we attached DSS images of the two dSphs, F8D1 and BK5N, studied by Caldwell et al. (1998).

2. HST WFPC2 photometry

The six dSph galaxies were imaged with the Wide Field and Planetary Camera 2 (WFPC2) aboard the Hubble Space Telescope over the interval August 14 – September 26, 1999, as part of an HST snapshot survey (program GO 8192, PI: Seitzer) of nearby dwarf galaxy candidates from the kk-list. The data were obtained with exposure times of 600 s in the F606W and F814W filters. Fig. 2 shows the galaxy images where both filters were combined. Each galaxy was centered on the WF3 chip. Two lines in the upper right corner indicate the North and East directions. In the case of DDO 78 the WF4 chip is overlit by a bright star.

Before the HST observations were obtained, two objects, K61 and K64, had been imaged with a CCD at the 6-meter telescope. Their images in the R band, each about $3'.1 \times 2'.7$ in size, are presented in Fig. 3. After removing cosmic ray hits we carried out point source photometry of the frames with the DAOPHOT II package by Stetson et al. (1990) implemented in MIDAS. The standard DAOPHOT/ALLSTAR procedure was used for automatic star finding and then measuring stellar magnitudes by fitting the point-spread function for each WF chip in each filter. A total of 1500 – 4000 stars/object were measured in both filters with an aperture radius of 1.5 pixels. Using bright isolated stars, we determined the aperture correction from the 1.5 pixel radius aperture to the standard $0'.5$ radius aperture size for the WFPC2 photometric system; this correction is in the range of 0.40 – 0.55 mag. Then we used equations (1a), (1b), and (3) from Whitmore et al. (1999) to correct the magnitudes for the charge- trans-

Fig. 4. Color-magnitude diagrams from the WFPC2 data for six dSph galaxies. The three panels for each galaxy show diagrams based on stars within the central (WF3) field, the "medium" field (the neighbouring halves of the WF2 and WF4 chips), and the outer field (remaining halves of the WF2 and WF4 chips). Each of these three fields covers an equal area of 800×800 pixels. The solid lines in the left panel show the mean loci of the red giant branches of globular clusters with different metallicities, M15 (-2.17 dex), M2 (-1.58 dex), and NGC 1851 (-1.29 dex.) from left to right, based on Da Costa & Armandroff (1990).

Fig. 5. Globular cluster candidates shown in the F606W+F814W filters from HST. In case of K64 the central background galaxy is presented.

fer efficiency loss, which depends on the X- and Y- positions, the background counts, the brightness of the star and the time of the observations. Transformation of the F606W and F814W instrumental magnitudes to the standard ground-based V, I system followed the prescriptions of Table 10 (here Holtzman et al. 1995) taking into account different relations for blue and red stars separately. Because we used a non-standard V filter F606W instead of F555W, the resulting V, I magnitudes may contain systematic zero-point errors, which are expected to be within 0.1 mag. Finally, objects with goodness of fit parameters $|\text{SHARP}| > 0.3$, $|\text{CHI}| > 2$, and $\sigma(V) > 0.2$ mag were excluded. The resulting color-magnitude diagrams (CMDs) in $I, V - I$ are presented for the six objects in Fig. 4.

3. Color-magnitude diagrams and distances

For each object the left panel of Fig. 4 shows the CMD for the central WF3 field covering the main galaxy body. The middle panel represents the CMD for the neighbouring regions in the southern half of WF2 and the eastern half of WF4 (the "medium" field), and the right panel comprises stars found in the remaining outer halves of WF2 and WF4. All six galaxy CMDs look rather similar to each other. Their stellar population is represented predominately by red stars. The number of stars in each central field rises steeply at I of about 23.9, which we interpret as the tip of the red giant branch (TRGB). All the galaxies show a significant number of red stars with $I < 23.9$, which could be upper asymptotic giant branch (AGB) stars. Their presence in these systems would not be surprising given that Caldwell et al. (1998) found them in much higher S/N WFPC2 observations of two other M81 dwarfs: F8D1 and BK5N. However, these AGB stars may also be due to a crowding effect (Grillmair et al. 1996, Martinez-Delgado & Aparicio 1997).

Either higher S/N data or a more sophisticated analysis of the current data would be required to establish the existence and quantity of AGB stars in these galaxies.

For metal-poor systems the TRGB may be assumed to be at $M_I = -4.05$ (Da Costa & Armandroff 1990). We find the apparent magnitude of the TRGB for different objects to be in the range of $I(\text{TRGB}) = [23.83 - 23.95]$, which yields distance moduli in the range of $[27.71 - 27.93]$ with Galactic extinctions A_I from Schlegel et al. (1998).

The individual values of $I(\text{TRGB})$, A_I , and $(m - M)_0$ for the objects are listed in Table 1. The solid lines in Fig. 4 are globular cluster fiducials from Da Costa & Armandroff (1990), which were reddened and shifted to the distance of each galaxy mentioned in Table 1. The fiducials cover the range of $[\text{Fe}/\text{H}]$ values: -2.2 dex (M 15), -1.6 dex (M2), and -1.2 dex (NGC 1851) from left to right. The last two columns of Table 1 refer to the objects F8D1 and BK5N studied by Caldwell et al. (1998). After correction for Galactic extinction from the IRAS/DIRBE results (Schlegel et al. 1998) their distance moduli, 27.88 and 27.89, lie in the same range as the others. As the one-sigma error of the derived distance moduli we adopt a value of $\sim 0^{\text{m}}15$, which includes a typical scatter in the TRGB position ($\sim 0^{\text{m}}1$) and an uncertainty of zero-points ($\sim 0^{\text{m}}1$) under "synthetic" transformations.

4. Metal abundances

Given the distance moduli of these dSph galaxies, we can estimate their mean metallicity, $[\text{Fe}/\text{H}]$, from the mean color of the TRGB measured at an absolute magnitude $M_I = -3.5$, as recommended by Da Costa & Armandroff (1990). Based on a Gaussian fit to the color distribution of the giant stars in a corresponding I -magnitude interval (-3.5 ± 0.3), we derived their mean colors, $(V - I)_{-3.5}$, which lie in a range of $[1.36 - 1.48]$ after correction for Galactic reddening. Following the relation of Lee et al. (1993), this provides us with mean metallicities, $[\text{Fe}/\text{H}] = [-1.27, -1.61]$, listed in Table 1. With a typical statistical scatter of the mean color ($0^{\text{m}}05$) and a probable systematic error in zero points and aperture corrections ($0^{\text{m}}10$) we expect an uncertainty in metallicity to be about ± 0.4 . Therefore within the measurement accuracy attainable with the photometric metallicity calibration the metallicity differences may not be significant, but we can certainly not rule out significant overall metallicity differences between the dSph galaxies in the M81 group.

5. Integrated properties

Apart from stellar photometry we also carried out aperture photometry of each galaxy in circular apertures, which allows some global parameters of the galaxies to be estimated: the color of the central part, the central

Table 1. Properties of dwarf spheroidal galaxies in the M81 group

Parameter	A0946+67 kk077	K61 kk081	D71=K63 kk083	K64 kk085	D78 kk089	BK6N kk091	F8D1 —	BK5N —
RA(1950.0)	09 46 08	09 53 01	10 01 18	10 03 09	10 22 48	10 31 00	09 40 45	10 00 45
D (1950.0)	67 44 25	68 49 47	66 48 00	68 04 19	67 54 32	66 16 00	67 42 20	68 29 54
$E(B - V)$	0.15	0.07	0.09	0.06	0.03	0.01	0.09	0.06
A_v	0.50	0.23	0.28	0.19	0.09	0.04	0.30	0.19
A_i	0.29	0.13	0.16	0.11	0.05	0.02	0.17	0.11
$a \times b(')$	2.4×1.8	2.4×1.4	1.7×1.5	1.9×0.9	2.0×1.9	1.1×0.7	2.2×2.0	0.8×0.6
V_T	15.5	14.2	14.9	14.6	15.1	16.0	15.0:	16.7
$(V - I)_T$	1.2	1.4	1.3	1.1	0.9	1.3	(1.1)	(1.0)
$\mu_v(0)$	24.7	23.5	23.3	23.3	24.5	24.2	25.4	24.5
$h('')$	25	32	22	21	28	18	54	12
$I_{(TRGB)}$	23.95	23.86	23.83	23.90	23.85	23.90	24.00	23.95
$(m - M)_0$	27.71	27.78	27.72	27.84	27.85	27.93	27.88	27.89
$(V - I)_{-3.5}$	1.62	1.48	1.60	1.47	1.42	1.39	1.61	1.36
$[Fe/H]$	-1.5	-1.6	-1.3	-1.5	-1.6	-1.6	-1.1	-1.7
D_{27} , kpc	2.6	2.6	1.8	2.0	2.1	1.2	2.3	0.8
M_v	-12.84	-13.87	-13.22	-13.43	-12.83	-11.88	-13.14	-11.33
$r(M81)$, (')	99	31	160	97	191	289	114	71
$R(M81)$, kpc	105	33	170	103	204	308	122	76
Type	dSph	dSph/dIrr	dSph	dSph	dSph	dSph	dSph	dSph
F , (mJy)	<5.5	<3.4	<3.4	<4.3	<4.9	<4.4	—	<3.6
N_{gc}	1:	1	1	0	1	1	1	0
S_N	7.4:	2.9	5.2	0	7.5	18.0	5.6	0

surface brightness, and the exponential scale length. Of course, the accuracy of these parameters is not high because of low surface brightness of the objects and because their extension is comparable to the WFPC2 field size. A summary of basic properties of the galaxies is given in Table 1. Its lines contain: (1,2) equatorial coordinates, (3–5) Galactic extinction from Schlegel et al. (1998), (6) galaxy dimensions along the major and minor axes approximately corresponding to a level of $B = (26.5 - 27.0)^m/\square''$, (7) integrated V magnitude estimated as an average of different sources, (8,9) integrated color of the central part and the central surface brightness from our measurements, (10) the exponential scale length in arcsec corresponding typically to a distance range of $[5 - 25]''$ from the galaxy center, (11) apparent I magnitude of the TRGB, (12) distance modulus, (13,14) the mean color of the TRGB and corresponding mean metallicity, (15,16) linear diameter and the total absolute magnitude of a galaxy, (17,18) angular and linear projected separation of galaxy from M81, (19) morphological type, (20) an upper limit of HI flux according Huchtmeier et al. (1999). The last two lines refer to galaxy globular cluster candidates (see the next section). For completeness we present also global parameters of two remaining dSph members of the M81 group: F8D1 and BK5N from Caldwell et al. (1998) after correction for the IRAS/DIRBE extinction. Note that these

authors estimated an apparent magnitude of F8D1 as $V_T = 13.85 \pm 0.25$, which makes it the brightest dSph in the M81 group. In Table 1 we adopt for F8D1 $V_T = 15.0 \pm 0.5$, based on the visual appearance of the object with respect to other dSphs.

Some additional comments about the galaxy properties are mentioned below.

kk77 = An0946+6745

Barely seen on the POSS-I prints because of a very low surface brightness, the object was discovered only on the POSS-II films (Karachentsev 1994). As with all other dSphs in the M81 group, kk77 has not been detected in the HI line (Huchtmeier et al. 1999).

K61 = kk81 = Mai47

This is the brightest dSph galaxy in the M81 group and also the closest companion to M81. After Karachentseva (1968) the object was rediscovered by Maillyan (1973) and Bertola & Maffei (1974). Its image and isodensity map were presented in the Atlas (Karachentseva et al. 1985) based on photographic observations with the 6-m telescope. According to these data K61 has a total magnitude $B_T = 15.6$ and a central surface brightness $\mu_B(0) = 24.4^m/\square''$ (Karachentseva et al. 1987). A photographic surface photometry made on the Tautenburg

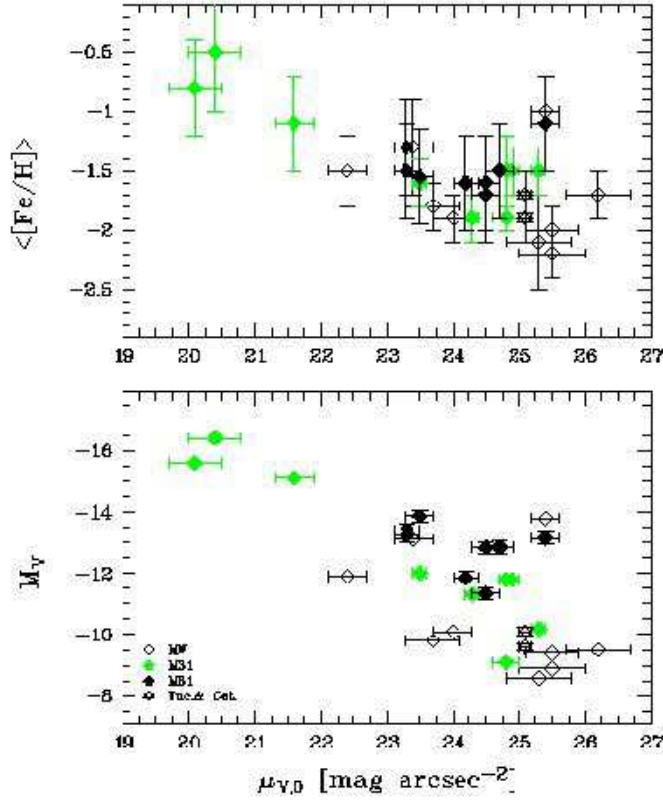


Fig. 6. Mean metallicity, $[Fe/H]$ (top), and absolute V magnitude, M_V (bottom), plotted vs. central surface brightness for dwarf spheroidal galaxies in the Milky Way + M31 group. The M81 dSphs (dark diamonds) follow the same overall relationship between these global properties as the LG dwarfs.

plates yielded $B_T = 14.9$, $V_T = 14.3$, $\mu_B(0) = 24.4$, and an exponential scale length of $h = 33''$ (Karachentseva et al. 1984). Bremnes et al. (1998) imaged K61 with a CCD at 1.2-m OHP telescope and derived the following parameters: $B_T = 15.25$, $R_T = 13.69$, $\mu_B(0) = 24.7$, and $h = 32''$, which are in a good agreement with the previous photographic data. Note also the results of CCD photometry of K61 by Johnson et al. (1997): $V = 15.68$, $R = 15.10$, and $I = 14.64$ referred to brighter ($26.0 - 26.5^m/\square''$) isophotes. The maps of neutral hydrogen emission in the vicinity of M81 show the presence of HI in the position of K61 (van der Hulst 1979, Appleton et al. 1981). Van Driel et al. (1998) have made a detailed analysis of all previous HI observations and their own. They note difficulties in HI searches for K61, because of the extended HI complex around M81 as well strong HI emission from our Galaxy. As a result, K61 was considered as having been undetected in the $(-260, +190)$ km s $^{-1}$ velocity range with a rms noise of 3.4 mJy. However, Johnson et al. (1997) revealed a bright HII knot situated

NE of the galaxy center. It shows a spectrum of high excitation with a radial velocity of -135 ± 30 km s $^{-1}$. As it is seen in Fig. 4, seven blue stars with $(V - I) < 0.4$ are observable in K61. Six of them are located in a small ($10'' \times 10''$) area coincident with the HII knot. Based on the presence of HII region and a probable presence of neutral gas, we assume K61 to be dSph/dIrr transition type.

DDO71 = K63 = UGC5428 = Mai49 = k83

Photometry of B plates obtained with the 6-m telescope gives for DDO 71 the following parameters: $B_T = 15.1$ and $\mu_B(0) = 24.3$. Its luminosity profile fits well the King model (Karachentseva et al. 1987). Bremnes et al. (1998) classified this galaxy as dE,N having an "off centre" nucleus. According to the 1.2-m CCD observations, they give $B_T = 15.95$, $R_T = 14.27$, the central surface brightness $\mu_B(0) = 24.3$, and the exponential scale length $h = 21''$. Huchtmeier & Skillman (1998) detected the galaxy in HI with a velocity of -126 ± 5 km s $^{-1}$ and a line

Table 2. Globular cluster candidates

Parameter	A0946+67 kk077	K61 kk081	D71=K63 kk083	K64 kk085	D78 kk089	BK6N kk091	F8D1 —	D44 kk061
V_T	22.83	20.70	20.95	(19.5)	19.45	21.80	21.68	22.18
$V - I$	0.95	1.10	1.11	(1.52)	1.11	1.24	0.76	0.83
$(V - I)_0$	0.74	1.00	0.99	(1.44)	1.07	1.22	0.64	0.77
$R(0.5L)$, (″)	0.45	0.20	0.26	(1.08)	0.30	0.29	0.18	0.27
$R(0.5L)$, pc	8.0	3.6	4.6	—	5.3	5.1	3.2	4.2
$\mu_v(0)$	22.4	18.5	19.2	(19.6)	18.0	20.2	20.2	20.8
M_v	-5.51	-7.37	-7.17	—	-8.48	-6.08	-6.46	-5.48
Separ., kpc	1.10	0.08	0.10	(0.12)	0.26	0.74	0.25	0.47

K64: The central diffuse object is not a globular cluster, but apparently background galaxy.

width of $W_{50} = 27 \text{ km s}^{-1}$. But van Driel et al. (1998) did not detect it at a rms noise level of 3.4 mJy; neither did Fisher & Tully (1981) or Schneider et al. (1992).

K64 = UGC5442 = Mai50 = kk85

Based on photometry obtained with the 2-m Tautenburg telescope plates (Börngen et al. 1982), the magnitude and $26.6^m/\square''$ isophote diameter are: $B = 15.5$, $a = 2'.0$, and $V = 14.7$, $a = 2'.1$. Later photometry by Karachentseva et al. (1984) gives $B = 15.7$ and $V = 14.8$. The same value, $B_T = 15.7$, was derived from photometry of the 6-m telescope plates. In the Atlas the galaxy shows a regular elliptical shape with an axial ratio of 0.5 and a low brightness gradient, without structural complexities and knots. The bright "nucleus" in its center was suggested as a foreground star. The luminosity profile of K64 is well fit an exponential law down to the $28^m/\square''$ level (Binggeli & Prugniel 1994). The CCD photometry by Bremnes et al. (1998) gives for K64: $B_T = 15.46$, and $R_T = 14.04$ with a central surface brightness and an exponential scale length, $\mu(0) = 24.2(B)$, $23.0(R)$, and $h = 21''(B)$, $23''(R)$, respectively. The object was surveyed in HI but not detected by Schneider et al. (1992), van Driel et al. (1998), and Huchtmeier & Skillman (1998).

DDO78 = kk89

According to Karachentseva et al. (1987), DDO 78 has a very flat surface brightness profile with $\mu_B(0) = 25.1$, $r_{ef} = 32''$, and $B(t) = 15.8$. It was not detected in HI by Fisher & Tully (1981) and van Driel et al. (1998). But observations with the 100-m Effelsberg radio telescope (Huchtmeier et al. 2000) yield an emission with $V_h = 2788 \pm 2 \text{ km s}^{-1}$ and a linewidth $W_{50} = 32 \text{ km s}^{-1}$, which is probably caused by a background galaxy.

BK6N = kk91

BK6N was discovered by Börngen and Karachentseva (1982) on the Tautenburg 2-m telescope plates. Its image

and isodensity map are presented in the Atlas, where BK6N has an elliptical shape with an axial ratio of 0.5, a very low surface brightness gradient without any structural details. Bremnes et al. (1998) presented an underexposed image of BK6N. Photographic photometry by Börngen et al. (1982) yields only a rough total magnitude estimate, $B_T = 15.7$; no more optical data were published. BK6N was not detected in the HI line by Huchtmeier & Skillman (1998) and van Driel et al. (1998).

6. Globular clusters

The brightest dSph galaxies in the Local Group contain globular clusters. Harris & van den Bergh (1981) proposed to describe their abundance by a specific frequency

$$S_N = N_{gc} \cdot dex[0.4 \cdot (15 + M_v)],$$

which is the number of observed globular clusters normalized to a galaxy with $M_v = -15$. According to Miller et al. (1998) nucleated and non-nucleated dE+dSph galaxies have specific frequencies of 6.5 ± 1.2 and 3.1 ± 0.5 , respectively.

We searched for globular clusters in our galaxies and found 5 candidates with appropriate colors and magnitudes. Their numbers per galaxy and corresponding specific frequencies are presented in the last two lines of Table 1. In Fig. 3 these candidates are indicated by circles. Enlargements of their HST images are given in Fig. 5. Table 2 presents basic photometric data for the globular cluster candidates. Its lines give: (1,2) integrated apparent magnitude and color, (3) integrated color after correction for Galactic reddening, (4,5) angular and linear half-light radius, (6) the central surface brightness, (7) integrated absolute magnitude, and (8) linear projected separation of probable globular cluster from the galaxy center. The last two column give similar parameters for another two dSphs in the group from Caldwell et al. (1998) and Karachentsev et al. (1999). All the globular cluster candidates have

integral colors $[0.64 - 1.22]$, absolute magnitudes $[-5.5 - -8.5]$, and half-light radii $[3.2 - 8.0]$ pc, which are within

values typical of Galactic globular clusters. All of them, except the kk77 candidate, show pronounced concentration towards the galaxy centers. Considering its excentric position, as well as its low central surface brightness, the globular cluster candidate in kk77 may be a background galaxy. The case of K64 needs also a special comment. Binggeli & Prugniel (1994) considered its central star-like object to be a "quasi-stellar nucleus". However, the large-scale HST image of it (Fig. 5) indicates that this object is a remote red galaxy. Therefore, both "nucleated" dSphs in M81 group: K 64 and BK5N (Caldwell et al. 1998) are instead probable non-nucleated spheroidal systems. For the total sample of 9 dSphs in M81 group their median specific frequency of globular clusters, $\langle S_N \rangle = 5.6$, agrees well with the data of Miller et al. (1998).

7. Subsystem of dSphs in the M81 group

Fig. 6 presents the distributions of dwarf spheroidal galaxies of the Local Group according to their absolute magnitude (lower panel) and metallicity (upper panel) versus the central surface brightness based on the data of Grebel (2000). Except for Sagittarius, the companions of the Milky Way (open diamonds) and M31 (grey diamonds) follow the well-known sequences that have been discussed by various authors (Lee 1995, Grebel & Guhathakurta 1999). Here the positions of 8 spheroidal companions of M81 are shown by dark diamonds. Except for F8D1 discussed by Caldwell et al. (1998), all dSphs of the M81 group follow the same common relations. However, one can note that the scatter of the M81 dSphs in the diagrams is not as great as for the LG dwarfs.

From the dynamical point of view it seems reasonable to consider the companions of MW and M31 as separate subsystems. The three giant spiral galaxies MW, M31, and M81 have the same morphological type, Sb, and approximately the same masses, $\sim (3 - 4)10^{11}M_{\odot}$, within the standard optical radius. All known spheroidal companions of them are presented in Table 3, where dSphs are arranged in order of their separation from the parent galaxy. According to these data each giant Sb galaxy has almost the same number of dSphs: 9, 8, and 8. The average and the maximum dimension of the three dSph subsystems do not differ significantly from one another. However, because the companions of MW have 3D distances, but not projected ones, the dimensions of dSph subsystems for M31 and M81 look a bit more extended. As one can see from the third column of Table 3, the mean luminosity of spheroidal companions of MW is much lower than for M81 companions. The difference in absolute magnitudes of dSphs for MW and M81 is significant at a 3σ level. Several reasons may be proposed to explain this difference.

a) When searching for dSphs in the M81 group, many very faint objects were missed. The faintest known spheroidal system around M81 has $M_v = -11.3$, but

Table 3. Projected separations and absolute magnitudes of dSph companions of Milky Way, M31 and M81

Milky Way			M 31			M 81		
Name	D, kpc	Mv	Name	D, kpc	Mv	Name	D, kpc	Mv
Sagittarius	24	-13.8	AndI	45	-11.8	K61	33	-13.8
Ursa Minor	66	-8.9	AndIII	67	-10.2	BK5N	76	-11.3
Sculptor	80	-9.8	N185	97	-15.6	K64	103	-13.4
Sextans	86	-9.5	N147	101	-15.1	kk77	105	-12.8
Draco	86	-8.6	AndV	109	-9.1	F8D1	122	-13.1
Carina	100	-9.4	AndII	141	-11.8	D71	170	-13.2
Fornax	140	-13.1	Cassiopeia	225	-12.0	D78	204	-12.8
LeoII	210	-10.1	Pegasus	278	-11.3	BK6N	308	-11.9
LeoI	250	-11.9						
Mean	116	-10.6		133	-12.1		140	-12.8
\pm	24	0.7		29	0.8		30	0.3
σ	68	1.9		78	2.1		80	0.8

the fraction of such faint objects among dSph companions of MW consists of 2/3. Therefore, assuming a similar luminosity function for both the groups leads to an expected total number of dSphs in the M81 group of ~ 24 . However, recent careful searches for new dSph objects in the vicinity of M81 have revealed only two new probable spheroidal dwarfs with $M_v \sim -10, -11$ mag (Karachentsev & Karachentseva 2000) and (Froeblich & Meusinger 2000). b) Another cause of the discussed difference may be systematic underestimate of the total apparent magnitudes for the most faint and diffuse companions of MW, like Ursa Minoris, Draco, and Carina. But the effect of underestimating must reach 2–3 mag, which seems to be quite improbable. c) Possibly the observed difference may be related to kinematic and dynamic features of the groups themselves such as interaction between M81 and M82.

8. Distribution of dwarfs in the M81/NGC2403 complex

The general distribution of galaxies in an extended vicinity around M81 is shown in Fig. 7 in supergalactic coordinates. The five largest galaxies with masses $\lg(M/M_\odot) > 10$ are indicated with large filled circles. Small filled and open circles denote irregular and spheroidal dwarfs, respectively. The numbers under the galaxy names correspond to their radial velocities in km s^{-1} with respect to the Local group centroid. A more detailed map of the central part of the group is given in the bottom panel of Fig. 7. According to the group membership criterion proposed by Karachentsev (1994), dwarf irregular galaxies NGC 2366, UGC 4483, Ho II, and K52 are associated with the Sc galaxy NGC 2403. Apparently DDO 44 is also one of its companions too (Karachentsev et al. 1999). A multiple system on the opposite side of M81 is formed by the Scd galaxy NGC 4236 and two irregular dwarfs, DDO 165 and UGC 7242. The remaining dwarf galaxies

in Fig. 7 are probable companions of M81, particularly, the most remote ones UGC 6456 (= VII Zw 403) and DDO 53.

We do not discuss here the dynamic state of the M81 group contemplating to do it as soon as accurate distances of all irregular galaxies in the group are measured. We note only the distinct effect of morphological segregation in the group: the median separations of dSphs and dIrrs from M81 have a ratio of 4:7. The same tendency is seen also for companions of NGC 2403 and for the Local Group. As Fig. 7 shows, the dwarf spheroidal galaxies are distributed around M81 asymmetrically. With respect to the group centroid (situated between M81 and M82) all 8 dSphs are concentrated in one quadrant. This feature may be explained by observational selection related to the presence of faint cirrus in the vicinity of M81 (see Fig. 4A in Bremnes et al. 1998), in which case 3/4 of the dSphs would be undetected, and their true number in the group would be about 32.

Estimates of distance moduli for members of the M81/NGC2403 complex measured via TRGB or cepheids are presented in Table 4. The original values of moduli were corrected for galactic extinction according to Schlegel et al. (1998) indicated in column (3). In all cases when TRGB method was applied we used a value of $M_I(\text{TRGB}) = -4.05$. For the six dwarf spheroidal galaxies studied here the mean distance modulus is 27.80 with a formal error of 0.04 mag. The true error may be 2–3 times larger, taking into account errors of photometric zero-points and also stellar crowding effect (Madore & Freedman 1995). Nevertheless, distance moduli for F8D1, BK5N, M82, and UGC 6456 derived via TRGB by other authors are in reasonable agreement with our data. Especially good agreement is found for the distance modulus for M81 measured by Freedman et al. (1994) via 30 cepheids. Thus, 11 members yield for the M81 group a mean distance modulus $(m - M)_0 = 27.84 \pm 0.05$ with a dispersion of individual estimates of only 0.15 mag. The last value corresponds for-

Table 4. Precise distance moduli for members of the M81/NGC 2403 complex

Galaxy	$(m - M)_0 \pm \sigma$	A_i	Method	Source
M81	27.70 ± 0.20	0.16	30 cephs	Freedman et al. (1994)
BK5N	27.89 ± 0.15	0.11	TRGB	Caldwell et al. (1998)
F8D1	27.88 ± 0.10	0.17	TRGB	Caldwell et al. (1998)
UGC6456	28.23 ± 0.10	0.07	TRGB	Lynds et al. (1998)
M82	27.74 ± 0.14	0.26	TRGB	Sakai & Madore (2000)
kk77	27.71 ± 0.15	0.29	TRGB	present paper
K61	27.78 ± 0.15	0.13	TRGB	present paper
DDO71	27.72 ± 0.15	0.16	TRGB	present paper
K64	27.84 ± 0.15	0.11	TRGB	present paper
DDO78	27.85 ± 0.15	0.05	TRGB	present paper
BK6N	27.93 ± 0.15	0.02	TRGB	present paper
Mean	27.84 ± 0.05			
NGC2403	27.49 ± 0.24	0.08	8 cephs	Freedman & Madore (1988)
DDO44	27.52 ± 0.15	0.08	TRGB	Karachentsev et al. (1999)
Mean	27.50 ± 0.02			

mally to the dispersion of radial distances of the galaxies, ~ 260 kpc, which is comparable with the projected linear dimension of the group.

The second subgroup of galaxies associated with NGC 2403 has only two accurate distance estimates (the last lines in Table 4), and they show excellent mutual agreement. Relying on these data, we conclude that there is a systematic difference in distance moduli between M81 and NGC 2403 subgroups of $+0.34 \pm 0.05$ mag. This means that NGC 2403 is situated 0.54 Mpc closer to us than M81. Fig. 8 shows a scheme of their location with respect to the Local Group. Note that the more distant galaxy M81 has a radial velocity lower than that of NGC 2403. To explain this fact we must assume that these galaxies have peculiar velocities directed towards each other. The difference of their radial velocities, -161 km s^{-1} , seems to be rather high. Part of it is probably caused by the motion of M81 with respect to M82. For the centroids of both subgroups the difference is -139 km s^{-1} (or -112 km s^{-1}) depending on whether the three unreliable velocity measurements (for BK3N, K63, and K73) are included or disregarded.

Therefore, one might think that the two subgroups around M81 and NGC 2403 have a spatial separation of 0.94 Mpc, and are approaching each other at a velocity of $\sim 110 - 160 \text{ km s}^{-1}$. Such a situation resembles the Local complex, where the Milky Way and M31 subsystems are separated by ~ 0.8 Mpc move towards each other at 120 km s^{-1} . Probably, the merger of tight binary groups is a common phenomenon on a scale of ~ 1 Mpc.

Acknowledgements. Support for this work was provided by NASA through grant GO-08192.97A from the Space Telescope Science Institute, which is operated by the Association of Universities for Research in Astronomy, Inc., under NASA contract NAS5-26555. IDK, VEK, and EKG acknowledge partial support through the Henri Cr  tien International Research Grant

administered by the American Astronomical Society. EKG acknowledges support by NASA through grant HF-01108.01-98A from the Space Telescope Science Institute. This work has been partially supported by the DFG-RFBR grant 98-02-04095.

This research has made use of the NASA/IPAC Extragalactic Database (NED) which is operated by the Jet Propulsion Laboratory, California Institute of Technology, under contract with NASA. We also used NASA's Astrophysics Data System Abstract Service and the SIMBAD database, operated at CDS, Strasbourg. The Digitized Sky Surveys were produced at the Space Telescope Science Institute under U.S. Government grant NAG W-2166. We thank the referee, A.Aparicio, for valuable comments.

References

- Appleton P.N., Davies R.D., Stephenson R.J. 1981, MNRAS 195, 327
- Appleton P.N., Siqueira P.R., Basart J.P., 1993, AJ 106, 1664
- Bertola F., Maffei P., 1974, A&A, 32, 117
- Binggeli B., Prugniel P. 1994, La Lettre de l'OHP, N.12
- B  rngen F., Karachentseva V.E., Schmidt R., Richter G.M., Th  nert W. 1982, Astron. Nachr. 303, 287
- B  rngen F., Karachentseva V.E. 1982, Astron. Nachr. 303, 189
- Bremnes T., Binggeli B., Prugniel P. 1998, A&AS 129, 313
- Caldwell N., Armandroff T.E., da Costa G.S., Seitzer P. 1998, AJ 115, 535
- da Costa G.S., 1988 in "Stellar astrophysics for the Local Group", Cambridge, Univ. of Cambridge Pres, 351
- da Costa G.S., Armandroff T.E., 1990, AJ 100, 162
- Fisher J.R., Tully R.B., 1975, A&A, 44, 151
- Fisher J.R., Tully R.B., 1981, ApJS 47, 139
- Freedman W.L., Madore B.F., 1988, ApJ, 332, L63
- Freedman W.L., Hughes S.M., Madore B.F., et al., 1994, ApJ, 427, 628
- Froebich D., Meusinger H., 2000, A&AS 145, 229
- Gebel E.K., 1997, Review of Modern Astr 10, 29

- Grebel E.K., 2000, in Star Formation from the Small to the Large Scale, 33rd ESLAB Symposium, eds. F.Favata, A.A.Kaas & A.Wilson (ESA: Noordwijk), in press
- Grebel E.K., Guhathakurta P., 1999, *ApJ*, 511, L101
- Grillmair C.J., Lauer T.R., Worthey G., Faber S.M., Freedman W.L., Madore B.F., Ajhar E.A., Baum W.A., Holtzman J.A., Lynds C.R., O'Neill E.J., Stetson P.B., 1996, *AJ* 112, 1975
- Harris W.E., van den Bergh S., 1981, *AJ*, 86, 1627
- Holtzman J.A., Burrows C.J., Casertano S., Hester J.J., Trauger J.T., Warson A.M., Worthey G., 1995, *PASP* 107, 1065
- Huchtmeier W.K., Skillman E.D. 1998, *A&AS* 129, 269
- Huchtmeier W.K., Karachentsev I.D., Karachentseva V.E., Ehle M. 2000, *A&AS* 141, 469
- Johnson R.A., Lawrence A., Terlevich R., Carter D. 1997, *MNRAS* 287, 333
- Karachentsev I.D. 1994, *Astron. Astrophys. Trans.* 6, 1
- Karachentsev I.D., Sharina M.E., Grebel E.K., Dolphin A.E., Geisler D., Guhathakurta P., Hodge P.W., Karachentseva V.E., Sarajedini A., Seitzer P. 1999, *A&A* 352, 399.
- Karachentsev I.D., Karachentseva V.E., 2000, *A&A*, in preparation
- Karachentseva V.E. 1968, *Commun. Byurakan obs.* 39, 62
- Karachentseva V.E., Schmidt R., Richter G.M., 1984, *Astron. Nachr.* 308, 247
- Karachentseva V.E., Karachentsev I.D., Börngen F. 1985, *A&AS* 60, 213 (Atlas)
- Karachentseva V.E., Karachentsev I.D., Richter G.M., von Berlepsh R., Fritze K. 1987, *Astron. Nachr.* 308, 247
- Karachentseva V.E., Karachentsev I.D. 1998, *A&AS* 127, 409
- Lee M.G., 1995, *AJ*, 110, 1129
- Lee M.G., Freedman W.L., Madore B.F., 1993, *AJ* 106, 964
- Madore B.F., Freedman W.L., 1995, *AJ* 109, 1645
- Mailyan N.A. 1973, *Astrofizika* 9, 33
- Martinez-Delgado D. & Aparicio A., 1997, *ApJ* 480, L107
- Mateo M., 1998, *A.Rev.A.A.* 36, 435
- Miller B.W., Lotz J.M., Ferguson H.C., Stiavelli M., Whitmore B.C., 1998, *ApJ* 508, L133
- Nilson P., 1973, *Uppsala Obs. Ann.* 6, 3 (UGC)
- Sakai S., Madore B.F., 2000, *ApJ* (in press)
- Sandage A.R., 1976, *AJ* 81, 964
- Schlegel D.J., Finkbeiner D.P., Davis M., 1998, *ApJ* 500, 525
- Schneider S.E., Thuan T.X., Mangum J.G., Miller J., 1992, *ApJS*, 81, 5
- Stetson P.B., Davis L.E., Grubtree D.R., 1990, in ASP Conf., Ser.8, CCDs in Astronomy, (San Francisco: ASP), 289
- van den Bergh S. 1959, *Publ. of D.D.O.*, v.II, N.5, 147
- van den Bergh S. 1966, *AJ* 71, 922
- van Driel W., Kraan-Korteweg R.C., Binggeli B., Huchtmeier W.K. 1998, *A&AS* 127, 397
- van der Hulst J.M., 1979, *A&A* 75, 97
- Whitmore B., Heyer I., Casertano S., 1999, *PASP*, 111, 1559

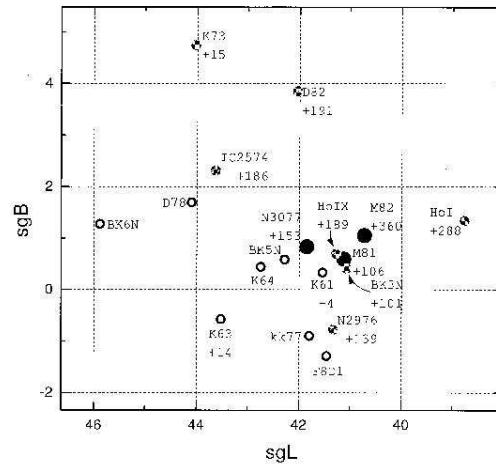
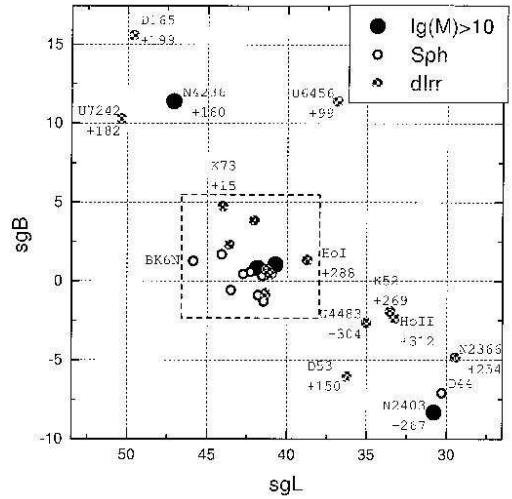


Fig. 7. The distribution of galaxies in supergalactic coordinates in the wide vicinity of the M81 group. Top: overview of the entire region, bottom: the central part of the M81 group.

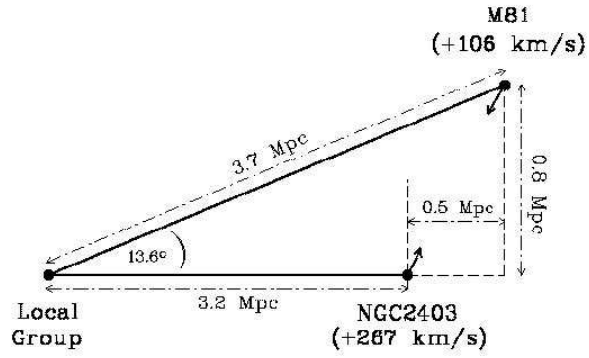


Fig. 8. A schematic disposition of M81 and NGC 2403 subgroups with respect to the Local group.

This figure "dwM81_f1.gif" is available in "gif" format from:

<http://arxiv.org/ps/astro-ph/0010146v1>

This figure "dwM81_f2a.gif" is available in "gif" format from:

<http://arxiv.org/ps/astro-ph/0010146v1>

This figure "dwM81_f2b.gif" is available in "gif" format from:

<http://arxiv.org/ps/astro-ph/0010146v1>

This figure "dwM81_f2c.gif" is available in "gif" format from:

<http://arxiv.org/ps/astro-ph/0010146v1>

This figure "dwM81_f2d.gif" is available in "gif" format from:

<http://arxiv.org/ps/astro-ph/0010146v1>

This figure "dwM81_f2e.gif" is available in "gif" format from:

<http://arxiv.org/ps/astro-ph/0010146v1>

This figure "dwM81_f2f.gif" is available in "gif" format from:

<http://arxiv.org/ps/astro-ph/0010146v1>

This figure "dwM81_f3a.gif" is available in "gif" format from:

<http://arxiv.org/ps/astro-ph/0010146v1>

This figure "dwM81_f3b.gif" is available in "gif" format from:

<http://arxiv.org/ps/astro-ph/0010146v1>

This figure "dwM81_f4a.gif" is available in "gif" format from:

<http://arxiv.org/ps/astro-ph/0010146v1>

This figure "dwM81_f4b.gif" is available in "gif" format from:

<http://arxiv.org/ps/astro-ph/0010146v1>

This figure "dwM81_f4c.gif" is available in "gif" format from:

<http://arxiv.org/ps/astro-ph/0010146v1>

This figure "dwM81_f4d.gif" is available in "gif" format from:

<http://arxiv.org/ps/astro-ph/0010146v1>

This figure "dwM81_f4e.gif" is available in "gif" format from:

<http://arxiv.org/ps/astro-ph/0010146v1>

This figure "dwM81_f4f.gif" is available in "gif" format from:

<http://arxiv.org/ps/astro-ph/0010146v1>

This figure "dwM81_f5a.gif" is available in "gif" format from:

<http://arxiv.org/ps/astro-ph/0010146v1>

This figure "dwM81_f5b.gif" is available in "gif" format from:

<http://arxiv.org/ps/astro-ph/0010146v1>

This figure "dwM81_f5c.gif" is available in "gif" format from:

<http://arxiv.org/ps/astro-ph/0010146v1>

This figure "dwM81_f5d.gif" is available in "gif" format from:

<http://arxiv.org/ps/astro-ph/0010146v1>

This figure "dwM81_f5e.gif" is available in "gif" format from:

<http://arxiv.org/ps/astro-ph/0010146v1>

This figure "dwM81_f5f.gif" is available in "gif" format from:

<http://arxiv.org/ps/astro-ph/0010146v1>